Original Article
ISSN (Online): 2582-7472

ShodhKosh: Journal of Visual and Performing Arts
July 2024 5(7), 677–689

DESIGNING OF MULTIFUNCTIONAL EV CHARGER BASED ON SOLAR PV ARRAY

S.Anusha[1], K.Nagabhushanam[2]

[1]Assistant Professor (Adhoc), JNTUA College of Engineering, Anantapur
[2]Assistant Professor (Adhoc), JNTUA College of Engineering, Anantapur

ABSTRACT

A grid operated by a sunlight concentrator system is developed for a domestic electric vehicle (EV) charger in this paper, it meets the requirements of an electric vehicle, home loads, and the grid. The charger will run independently, employing a solar panel to give uninterruptible charging and control of home loads. The grid connected mode of operation is available in the absence of a Photovoltaic panel or when the Photovoltaic module's power is unsatisfactory. In addition, the charger is assisted by the synchronized and smooth phase shifting control, which allows it to immediately connect and disconnect from the grid, neither interfering with EV charging nor home supplies. Moreover, the battery is allowed to support grid and vehicle-to-home (V2H) power transmission with vehicle-to-grid (V2G) active/reactive power support to support local loads in island conditions. The battery is often regulated to perform as an active power filter, ensuring that the grid current has a unity power factor (UPF) and a total harmonic distortion (THD) of less than 5 percent. The battery is intended for use with a 1 – Ø 230V 50Hz and by using MATLAB/Simulink software to validate the simulation results.

Keywords: Electric Vehicle (EV), Vehicle-to-home (V2H), Vehicle-to-grid (V2G), Grid connected mode control (GCMC), Islanded Mode Control (IMC)

Corresponding Author

S. Anusha,
sankranthi.anusha2425@gmail.com

DOI
10.29121/shodhkosh.v5.i7.2024.4307

Funding: This research received no specific grant from any funding agency in the public, commercial, or not-for-profit sectors.

1. INTRODUCTION

EVs are becoming more popular as a viable remedy to the difficulties produced by conventional energy sources cars in the current environment [1]. The flexibility of electric vehicles, on the other hand, is determined by charging infrastructure [2]. Charging an electric vehicle needs a large quantity of electric power it is generated primarily from Coal or fuel generators. As a result, compared to the present vehicle framework, When the electrical energy required for EV charging comes from environmentally favorable power resources like sunlight arrays, wind, EVs can be a sustainable and smart option. For example, [3]. The solar panels electricity is generated and used locally, which is a benefit of such type of a power outlet. As a consequence, there is no need to rebuild transmission lines to meet the additional power. Furthermore, when energy costs are high, there is no need for a power outlet electricity from the network. Another advantage of a power outlet based on a sun powered module is completely space constrained. Ma et al recommend using an office building and a halting area to install sun-powered Photovoltaic module, as these sun-

powered Photovoltaic modules also act like a shade and protect vehicles and structures from overheating [4]. As a result, using a charging station based on a PV array not only avoids grid overloading, but it also saves money. It does, however, keep the charging station's operational costs to minimum. Furthermore, the PV exhibits scheduled activity reduces the effects of Photovoltaic power on the utility, and it eliminates the problems caused by Photovoltaic power irregularities caused by sunlight [5].

To connect the Photovoltaic module towards the dc interface, a dc-dc converter (often referred to as a support converter) is employed. The primary benefits of such location contain a minimization in one force stage due to the exclusion of the dc-dc converter stage, circuit complexity, and converter cost, all while maintaining the PV array's presentation. Unless the battery is only utilized to charge the Electric vehicle, the battery will be dormant fits over half of its life. As a result, while the EV isn't connected for charging, the charger's converter must be used for other projects in order to improve the charger's functional competence. Several functions are offered in the work, including four-quadrant charger activity, vehicle-to-home activity utilizing an EV battery, and dynamic separation, among others. [13].

A variety of converters and regulators are employed for distinct types of action in the available writing. Furthermore, network accessibility (islanded or lattice linked activity), methods of performance swapping among various working methods (consistent or irregular), and such variables all have an impact on the charger's functional competence. Many attempts are being made to develop an integrated framework that can carry out the leading capabilities that benefit the grid, family stacks, and electric vehicles. [14]. A family load included; matrix associated sun powered Photovoltaic module based Electric vehicle battery with various functionalities is carried out in this paper with the consolidated control for achieving the acceptable activity of many functions like i) Photovoltaic with Maximum power point tracking without the need of a dc-dc converter ii) charger activity in multi quadrants (G2V/V2G), iii) Non - linear burden on Vehicle to home, iv) dynamic separating, v) grid associated activity/islanding, vi) parallelism (programmed method exchanging), vii) Maximum power point tracking derating, viii) point of common coupling voltage rectification, and so on. Furthermore, connecting Electric vehicle battery charging with a sustainable energy resource, residential burden, and network causes issues for total energy management.

Table 1: State of Art on Solar PV based EV Charger

S.No.	References	PV array without dc-dc converter	Four quadrant operation (V2G/G2V)	V2H with nonlinear loads	Active filtering	Islanded/grid connected	Synchronization (Automatic mode switching)	MPPT Derating	PCC Voltage correction
1	[23],[12],[27],[10],[11],[29],[38],[4]	No	No	No	No	Grid Connected	No	No	No
2	[24]	No	No	No	No	Both	Yes	No	No
3	[25],[26]	No	No	No	No	Both	No	No	No
4	[9]	No	No	No	Yes	Grid Connected	No	No	No
5	[28],[30],[31],[32],[33],[35]	No	Yes	No	No	Grid Connected	No	No	No
6	[34]	No	No	Yes	No	Both	No	No	No
7	[36],[37]	No	No	No	No	Islanded	No	No	No
8	[39]	No	No	No	No	Islanded	No	Yes	No
9	[40]	No	Yes	Yes	No	Both	Yes	No	No
10	Proposed system	Yes	Yes	Yes	Yes	Both	Yes	Yes	Yes

A unique grid-integrated microgrid energy management system based on predictive fuzzy reasoning, where the controller uses the system's long-term model to estimate energy output, demand, and cost [26]. Many experts have planned to build an energy management system based on rules and optimization. A sliding mode control (SMC) is utilised in this work for dc-link voltage management, which enhances the system's dynamic and steady-state efficiency. SMC is recognised for its strong response and vigour in the face of disadvantages, such as opaque control variables and system limits [51]. In a single Electric vehicle battery structure, this work integrates multiple tasks, for example i)Photovoltaic with Maximum power point tracking without the need of a dc-dc converter ii) charger activity in multi quadrants (G2V/V2G), iii) Non - linear burden on Vehicle to home, iv) dynamic separating, v) grid associated activity/islanded, vi)parallelism (programmed method exchanging), vii) Maximum power point tracking derating, viii) Point of common coupling voltage .The benefit of this system is that it satisfies the needs of the residential load, the electric vehicle, and the utility all in one package.

The following are the key characteristics of this system:

- In grid-coupled and standalone method, the use of PV array energy for EV charging and home load control.
- At PCC, a strong control approach for producing a sinusoidal voltage with total harmonic distortion (THD) under 5% has been improved.
- The VSC and the EV battery combine to provide Vehicle-to-grid (V2G) reactive power under consumption.
- Implementing vehicle-to-home (V2H) work to provide the home demand in standalone method while utilizing EV battery energy.
- Control for synchronising grid and PCC voltages, as well as logic for producing switch enabling logic (E) with a smooth transition from standalone to grid coupled method.
- So that the charger does not contaminate the grid, it uses VSC as an active power filter.
- The IEEE-519 standard is always followed in grid coupled method for current and voltage.
- Ability to work effectively in a distorted voltage situation.
- For all operational modes, an energy management technique according to dc interface voltage control.
- The energy regulation method uses a SMC according to dc-interface voltage control to achieve the specified goals.

2. NETWORK DESIGN OF THE SYSTEM

Figure 1 illustrates the circuit architecture of the projected charge controller. This is a single-stage bi-directional battery for an electric vehicle it includes a sun-powered photovoltaic module a directly on the VSC's dc-link. This technology charges the electric vehicle charger utilizing sun- powered photovoltaic/grid electricity and transmits the sun-powered photovoltaic/Electric vehicle battery power back into the grid. This battery contains two stages, such as Conversion from ac to dc in both directions, then dc to dc in both directions. While charging the EV battery, the data is converted from AC voltage to DC voltage at the AC DC conversion stage and works as an inverter to convert the DC voltage to AC voltage while managing PV power and EV output into the grid. The output of bi-directional DC-DC converter is connected to the EV battery. The various tasks are completed by by the dc-dc converter in this battery. The DC converter operates in buck mode when charging the EV battery and in boost mode while discharging.

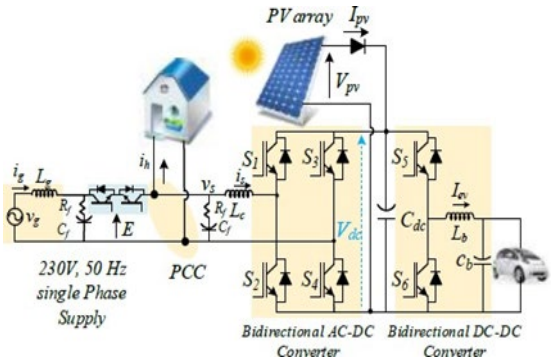

Fig. 1: Network Design Of The System

It also controls the DC bus voltage and ensures that the solar PV array generates the greatest amount of electricity possible. Through the coupling inductor, the charger is coupled to the grid (Lc). Harmonics must be removed, and the

grid current must be smoothed. To avoid the injection of switching harmonics generated by the VSC into the grid, a ripple filter is additionally linked at Point of Common Coupling.

3. STRATEGY FOR MANAGEMENT OF ENERGY

This charger's energy management technique is based on constant dc-link voltage control. Fig. 1 shows energy management flow chart under various operating circumstances. The steady-state is provided like this,

$\pm P_B \pm P_g - P_h + P_{PV} = 0$ (1)

Sun-powered modules power, Electric vehicle power, home load power, and grid power are all represented as P_{PV}, P_{EV}, P_h and P_g, respectively. The positive power in this equation denotes power supply, whereas the negative power denotes power consumption. This implies that both the EV and the grid can produce and consume electricity. The charger experiences a transient induced by Solar irradiation, household load, and Electric vehicle battery current are all increasing. when it is linked to the grid. The charging and discharging of the EV battery, as well as the home supply, should be unaffected by the PV array change in power.

As a result, during irradiance change, a sequence of processes takes place in order to achieve energy balance in the system.

Solar irradiance ↑↓→ P_{pv} ↑↓→ power at DC link ↑↓→ V_{dc} ↑↓→ V_{dc}regulation → I_p ↑↓→ I^* ↑↓→ I_g ↑↓ (2) g

Similarly, by the change in EV charging/discharging, and the sequence of The following are the energy management events that occur during this transient:

Charging power ↑↓→ I_{EV} ↑↓→power at direct current link↑↓→ V_{dc} ↑↓→ V_{dc} regulation→ I_p ↑↓→ I^* ↑↓→ ↑↓ (3)

g g

Energy management in a steady-state scenario in standalone mode is defined as

$P_{PV} \pm P_{EV} - P_h = 0$ (4)

Changes in solar irradiance and house load stop the energy flow in standalone mode, just as they do in grid linked mode. Because the dc-link voltage is controlled by the EV battery, it compensates for all power fluctuations. Changes in solar irradiation lead to energy management in the following ways:

Solar irradiance ↑↓→ P_{PV} ↑↓→ power at DC link ↑↓→ V_{dc} ↑↓→ V_{dc}regulation → I^* ↑↓→ I_{EV} ↑↓ (5) EV

Energy management is achieved whenever the home load changes.

i_h ↑↓→ power at direct current link P_{PV} ↑↓→ V_{dc} ↑↓→ V_{dc}regulation → I^* ↑↓→ I_{EV} ↑↓ (6) EV

4. ALGORITHM OF CONTROL

The control goal is to charge the electric vehicle and power the house without interruption, regardless of the circumstances. As a result, the control is structured in such a way that the multifunctional task is completed. As shown in Fig. 2, the control may be divided into two types: mode (islanded and grid linked). These two major controllers, however, encompass the vehicle- to-grid (V2G) dynamic and receptive forces, as well as the vehicle-to-home (V2H) modes. Also, It is described how to control a consolidated bi-directional dc-dc converter in both islanded and grid linked mode.

Fig. 2. Energy management flow chart

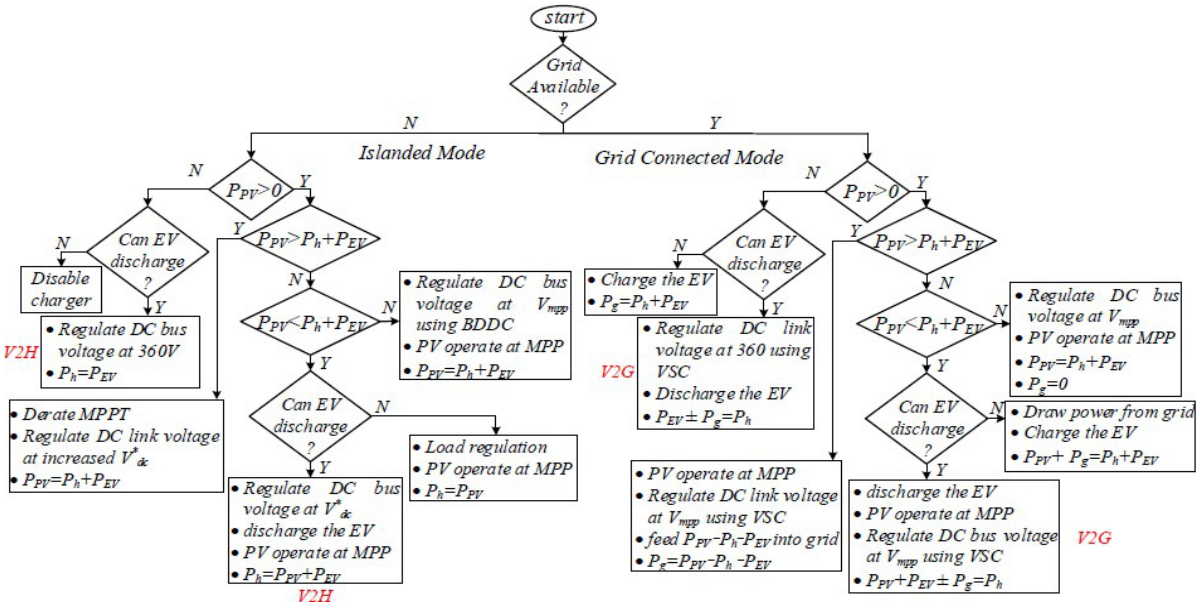

A. GRID CONNECTED MODE CONTROL.

The aim of GCM mode is to control the dc link voltage as well as the grid current in order to control the active and reactive power flow and, as a result, to generate the VSC exchanging beats. The following explanations are provided for sliding mode control (SMC) and variable speed control (VSC).

1) MODE OF SLIDING CONTROLLING THE VOLTAGE ON THE DC LINK

Sliding mode control is used to control the direct current -link voltage and MPPT of a sun-oriented photovoltic module in this paper. In single-stage geography, MPPT is performed by controlling the dc-interface voltage at the MPP voltage of the sun-powered PV exhibit, so the dc-interface voltage guideline is also required for the MPPT of the sunlight-based PV array.

The MPPT calculation [52] gauges the reference dc-connect voltage (V^*) at which the pinnacle force of the The solar-powered PV display has been dismantled. Regardless, in the absence of a sun-based PV age, the dc-connect voltage is controlled at a certain voltage (360V). The surface of the sliding mode control is designed using a combination of corresponding and basic parts of voltage error because the dc-connect voltage is directed by the SMC. To regulate the coming to and sliding elements of the machine, the corresponding and essential type of sliding surface is chosen
The voltage error is calculated as follows:

$$e= V^* - V_{dc} \quad (7)$$

sliding surface is given as,

$$S=\alpha_1 e + \alpha_2 \int_0^t e\,dt = \gamma e + \int e\,dt \quad (8)$$

Where, γ ($\gamma = \alpha_1/\alpha_2$) is a positive steady, which selects the regulator's consistent state and dynamic displays steady state inaccuracy, overshoot/undershoot, settling time, and vigour are only a few examples. The net active power flow determines the dc-voltage interface. When the net prompt active power flow increases, the dc-interface voltage rises. Regardless, when net negative prompt active power flow occurs, the dc-connect voltage decreases. As a result, the dynamic force balance in the system may be controlled in this manner. The assessment of the unpleasant portion of the reference system current and the dc-connect voltage guideline must be quick. the error is used as the sliding surface, which is based on the net dynamic force stream. The current estimated is given as

$$I_d = \begin{cases} P_{dc}^+ , S > 0 \\ P_{dc}^- , S > 0 \end{cases} \quad (9)$$

The SMC considers the first-order derivative of the dc-link voltage created by the power balancing at dc-link as follows:

$$P_{dc} = i_{dc} = C_{dc} V_{dc} \frac{d}{dt}\left(\frac{V_{dc}}{d_c}\right) + \frac{1}{R_L} V_{dc}^2 \quad (10)$$

On the charger's dc side, R_L is the equivalent load, which is simplified by modelling it as a resistive load. Using (9) and (10), the first-order derivative of the dc-link voltage may now be computed as follows:

$$V_{dc} = \frac{I_d}{C_{dc} V_{dc} d_c} - \frac{1}{R_L C_{dc} d_c} V_{dc} + \mu \quad (11)$$

Where variations in irradiance, load, and charging/discharging current cause a change in the dc- link voltage.
The controller for direct current-link voltage management and calculating the current loss component is built using Lyapunov stability criteria, which say that [53],

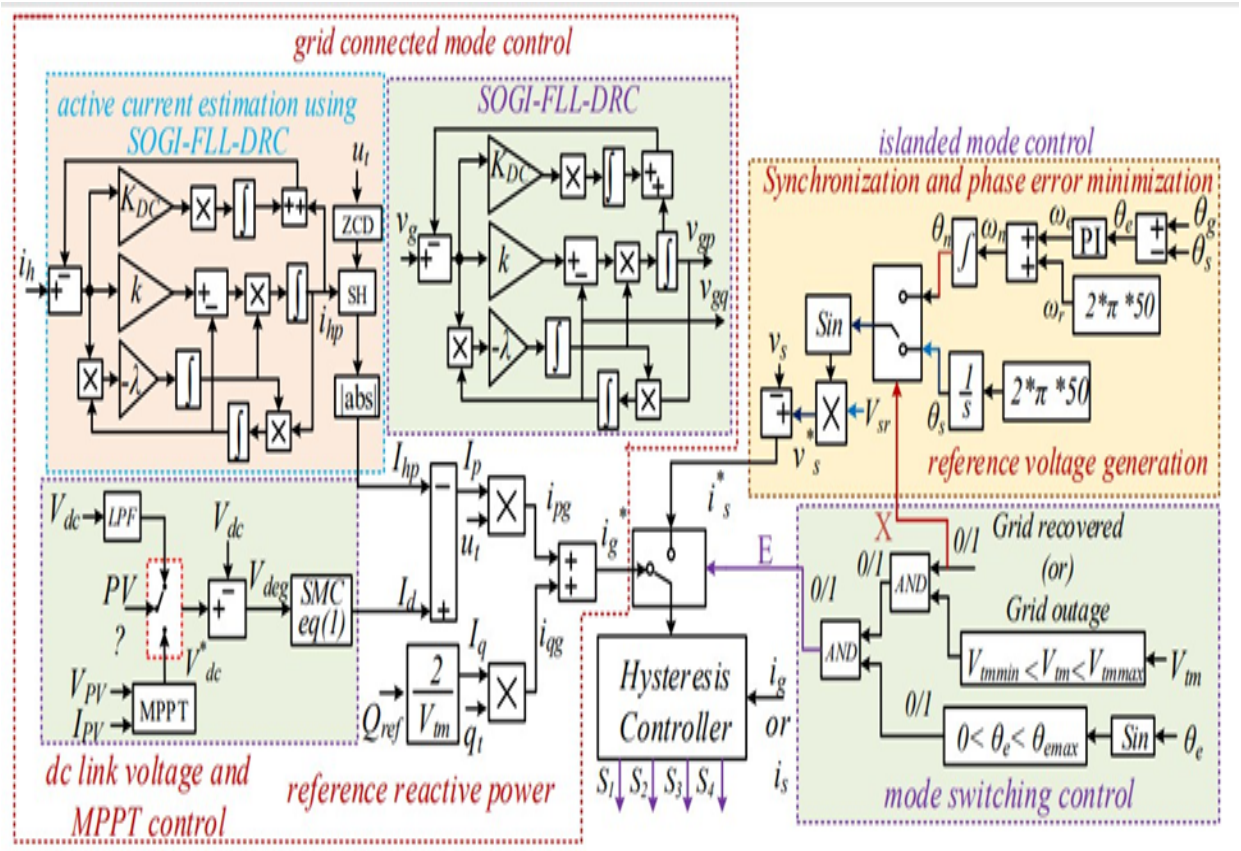

Fig. 3 Combined control strategy of VSC

$$\lim_{x\to 0} S.\dot{S} < 0 \qquad (12)$$

$$S\{\gamma(\dot{V_{dc}} - \dot{V_{dc}^*}) + e\} = S\{\gamma(\dot{V_{dc}}) + e\} \qquad (13)$$

$$S\left\{\gamma\left(\frac{I_d}{C_{dc}V_{dc}} - \frac{1}{R_L C_{dc}}V_{dc} + \mu\right) + e\right\} \qquad (14)$$

$$S\left\{\left(\frac{\gamma I_d}{C_{dc}V_{dc}} - \frac{\gamma}{R_L C_{dc}}V_{dc} + \gamma\mu\right) + e\right\} \qquad (15)$$

Now, I_d is select such that $S.\dot{S} < 0$

$$I_d = C_{dc}V_{dc}\left[\left(\frac{1}{R_L C_{dc}} - \frac{1}{\gamma}\right)V_{dc} + \frac{1}{\gamma}V_{dc}^* - (\sigma + \delta)\text{sign}(S)\right] \qquad (16)$$

If is a positive constant, then is also a positive constant. Appendix I contains the values of, and, which were chosen for implementation. In addition, Appendix II discusses the precise derivation of the controller's stability.

The chattering phenomena may emerge with the applied SMC control due to the existence of (σ+δ)sign(S) in (16). With the SMC control in place, the chattering cannot be completely eradicated. The chattering, on the other hand, has been restricted to a constant frequency by limiting the value of such that the (σ+δ) does not get too tiny. is defined as follows since is a positive constant

$$\delta = \begin{cases} ||e|| & , v_e > 0.1V \\ .1 & v_e < 0.1V \end{cases} \qquad (17)$$

2) GCM's VSC Control

Figure 3 depicts the VSC control. The grid current comprises harmonics as a result of non-linear home loads and the EV. Grid current also contains harmonics. Furthermore, the power factor (PF) deteriorates. As a result, a second-request summed integrator frequency locked circle with dc dismissal ability (SOGI-FLLDR) [54]is used to appraise the basic burden current so that the reference current is free of noises for working on the PF and ensuring the grid current THD inside 5%. Figure 3 demonstrates the extraction of the essential dynamic burden current component using a Zero Crossing Detector as an example. [54] is the articulation for the dynamic current assessment.

(18)

$$\frac{i_{hp}}{s^2} = \frac{}{k\omega}$$

$$i_h \qquad s^3+(k_o+k\omega)s^2+\omega^2(s+k_o)$$

The total active current is calculated to be as follows:

$$I_p = I_d - I_{hp} \qquad (19)$$

The amplitude of the reactive current (I q) of the reference grid current (i s*) is computed and given as part of the reactive power instruction (Q ref).

$$I_q = \frac{2\times Q_{ref}}{V_{tm}} \qquad (20)$$

To get instantaneous reference active grid current (I_p) and instantaneous reference reactive grid current (I_q), the actual (I_p) and reactive (I_q) components are multiplied by the in-phase (u_t) and quadrature-phase unit template (q_t), respectively.

The following equations provide the in-phase (u_t) and quadrature-phase (q_t) unit templates:

$$u_t = \frac{v_{gp}}{V_{tm}} \ , q_t = \frac{v_{gq}}{V_{tm}} \qquad (22)$$

Where $v_{gp}$and v_{gq} are the PCC voltage's in-phase and quadrature-phase voltages, respectively, and V_{tm} is the voltage's amplitude. These two (v_g and$v$) voltages acquired with the SOGI- FLLDR method become harmonic-free, resulting in sinusoidal approximated unit templates. The
V_{tm} may be calculated using v_{gp} and v_{gq} as follows:

$$V_{tm} = \sqrt{v^2 \ + v^2} \qquad (23)$$

The total reference grid current is calculated by multiplying (i_p) by reactive grid current (i_q).

$$i^* = i_p + i_q \qquad (24)$$

The hysteresis controller creates the triggering signals for the VSC after comparing the reference grid current (i^*) with the measured grid current (i).

B. IN STANDALONE MODE, VSC CONTROL

The integrated framework's goal in islanded mode is to charge the EV and provide the family load self-sufficiently using PV display energy. In addition, the V2H power mode is employed to meet the family load in the absence of PV exhibit energy. The VSC is regulated to function as an inverter to feed the heap in islanded mode, according to the control shown in Fig. 3. As shown in Fig.3, the regulator generates the voltage by using the reference recurrence and reference voltage. The VSC beats are generated using the measured voltage and the reference voltage. The charger should be coupled with the lattice for two-way power transfer while functioning in islanded mode. It is therefore necessary to synchronize the lattice voltage, recurrence, and stage with the PCC voltage, recurrence, and stage. The objective is for the matrix's association to become constant and programmed. The regulator evaluates the stage points of the PCC voltage and the lattice voltage in this manner, calculating the stage difference between the two voltages. To minimize the stage error between two voltages, the PI regulator is used The PI regulator decodes the stage mistake data and converts it into error recurrence. The regulator generates the reference voltage of rectified Recurrence using the error recurrence. When the periods of two voltages coincide, the regulator generates an enabling signal for the bidirectional switch using the exchange logic shown in Fig.3.

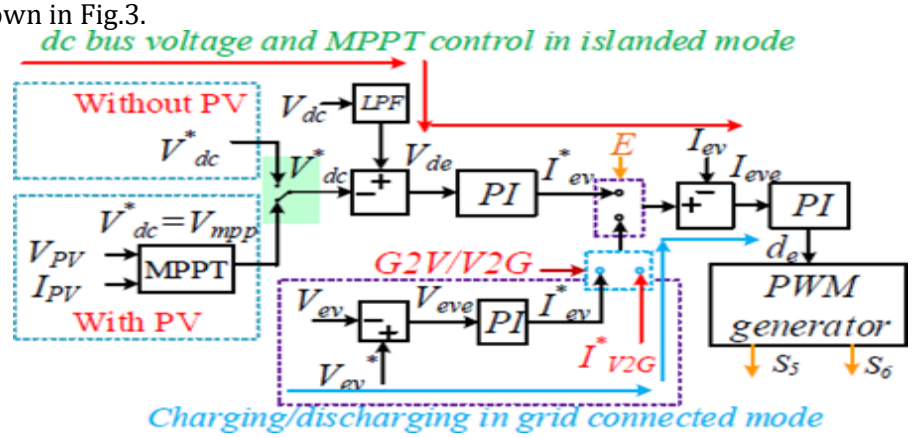

Fig 4: For bi-directional dc-dc converters, a combined control technique is used.

C. BDDC CONTROL

Using a PI regulator, the reference current is provided as,

$$I^*_{ev}(r) = I^*_{ev}(r-1) + k_{pv}\{V_{eve}(r) - V_{eve}(r-1)\} + k_{iv}V_{eve}(r) \quad (25)$$

Where V_{eve} is the dc-interface voltage mistake and k_{pv}, k_{iv} are the increases of the proportional integral regulator The client provides the reference current for releasing the EV battery in the V2G power transfer. It's worth noting that the V2G mode's display of reference EV current is the inverse of the G2V mode. The error in the EV current is now computed using the reference EV current and the observed EV flows, and the inward PI control produces the bi-directional dc-dc converter's obligation pattern. The obligation cycle is calculated as follows:

$$d(r) = d^*(r-1) + k_{pd}\{I_{de}(r) - I_{de}(r-1)\}k_{id}V_{de}(r) \quad (26)$$

In any instance, the dc-connect voltage is aimed towards a present voltage (V dc*=360V) without the PV exhibit (V2H), as shown in Fig. 4. In this case, too, a fell PI controller is used, with the exterior circle controlling the dc-interface voltage and the inner circle controlling the EV charging/releasing current. The exterior circle's statement is as follows:

$$I^*_{ev}(r) = I^*_{ev}(r-1) + k_{pd}\{V_{de}(r) - V_{de}(r-1)\} + k_{id}V_{de}(r) \quad (27)$$

The voltage error is represented by V_{de}. The profits of the controller, on the other hand, are k_{pd} and k_i. calculates the duty cycle based on the reference and measured current. The PWM generator then provides switching signals to the converter.

A. STEADY-STATE PERFORMANCE

Fig. 5 (a)- (b) show that the sun powered PV exhibit is creating 3.77kW. Out of 3.77 kW, 0.8kW is taken by the home load (P_h) and 0.95kW is utilized by the EV for charging

UPF manages the remaining1.91kW in the network. The voltage (V_{PV}), and home load voltage (V_h) of the sun powered PV exhibit are displayed in Fig. 5(a)- (b). The voltages, flows and powers of the heap and the (THD) In addition, it is likewise not drawing any receptive force from the grid as legitimized by EV battery are displayed in Fig 5 (c)-(d). The voltage (v_g), current (i_g), THD of the grid current (i_g) are shown in Fig. 5 (e).

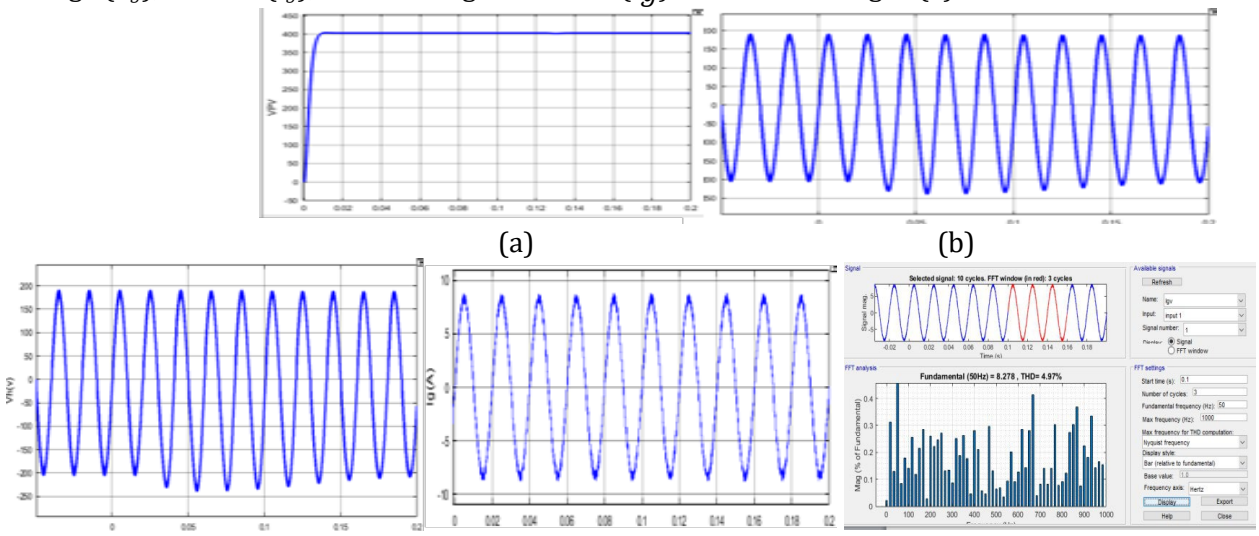

Fig 5: Steady state execution in GCM, (a)-(b) PV array voltage and home load voltage, (c)-(d) grid voltage and grid current, (e)total hormonic distortion of grid current.

A. DYNAMIC EXECUTION OF CHARGER

The islanded technique of the charger is provided to demonstrate the charger's capacity to function autonomously by employing sun-oriented PV cluster energy for EV charging and household load supply. The family load fluctuates as the solar powered irradiance changes during the islanded way of activity. As a result, Fig. 6 depicts the charger's operation under these disturbing effects. At first, the sunlight-based PV cluster charges the EV and feed the family load as displayed by the negative EV current in Fig. 6(a). Nonetheless, after some time, the sun-oriented PV array age.

(P_{PV}) becomes zero. Consequently, to take care of the heap uninterruptedly, the EV battery begins releasing, to support the home burdens, as displayed by the positive battery current (I_{ev}) in Figure 6 (a). This method is referred to as "vehicle to home." The voltage generated at the PCC (vs) using the charger is shown in Fig. 6 (b). Fig 6(a)-(b)dynamic execution of battery Notwithstanding, when the sun-oriented irradiance is expanded from 500W/m2 to 1000W/m2, the sun-based PV cluster age doesn't increment in light of the fact that the regulator expands the reference dc-connect voltage

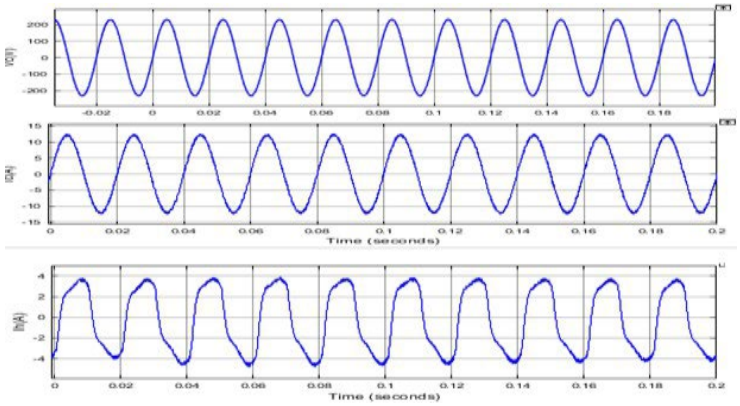

to accomplish the MPPT derating as the charging pace of EV is limited by the regulator as displayed in Fig. 6. The charger works in grid coupled method either due to the overabundance power age or force shortage. In the two cases, the charger trades the force with the framework at solidarity power factor. Nonetheless, in framework associated method additionally, numerous unsettling influences happen during the activity. Subsequently, the charger's constant activity is necessary in this functioning situation. In GCM, the behaviour under the heap problem is seen in Fig. 7. The dc- connect voltage is handled by the charger's voltage source converter in lattice associated mode, thus the heap change only affects the lattice power. The heap is modified in steps here, and the resulting difference in grid power (P_g) is shown in Fig. 7. (a). As seen in, a drop in load current (i_h) causes an increase in grid current (i_g), while the PV exhibit current (I_{PV}) and the Electric vehicle current (I_{EV}) do not. Irradiation from the sun is progressively lowered from 1000W/m2 to 700W/m2, then to 300W/m2, and so on. As a result, the grid power (P_g) is now both positive and negative. Excess energy is sent back into the grid at a rate of 1000W/m2. However, the electricity comes from the grid at a rate of 300W/m2. At P_g = 0k, Fig. 8 depicts the V2G responsive force execution. The grid current (I_g) goes from being trailing to leading when the reference receptive force (Q_{ref}) changes from 1kVAR to Minus 1kVAR. Dc-interface voltage (V_{dc}) is also unaffected. The charger's symphonies pay and PCC voltage remedy capacity are shown in Fig. 9. Without harmonic moderation, the grid current ($_g$) is identical to the home current (i_h) in Fig. 9. Nonetheless, the grid current (i_g) is seen to acquire a sinusoidal get-togethers remuneration. In Fig. 9, the current (i_s) of VSC is shown. Additionally, owing to remuneration, the PCC voltage (v_g) profile seems to be active After synchronisation, Fig. 10 illustrates the presentation of mode swapping control and empowering signal (E) age. The charger is spontaneously switching modes between islanded and grid connected modes, as seen in Fig. 10.

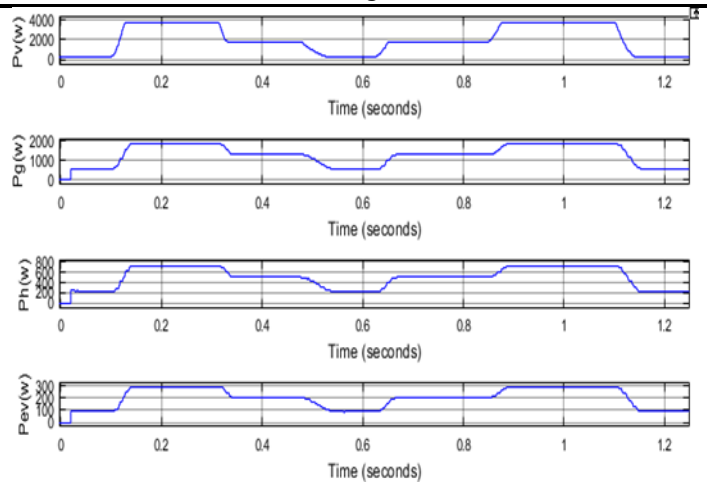

Fig .7 Variation in the output of sun illumination

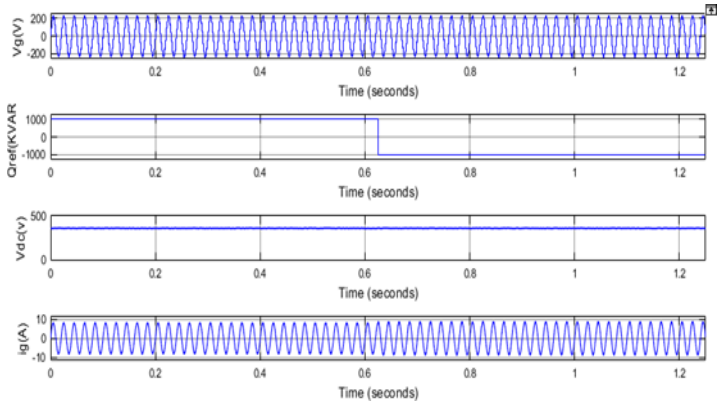

Fig.8. Performance of reactive power support from vehicles to the grid

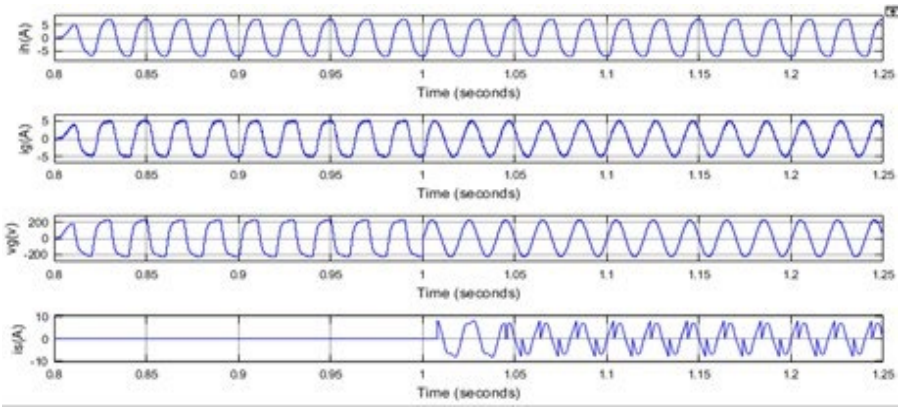

Fig .9. With an active power filter and in a distorted voltage scenario

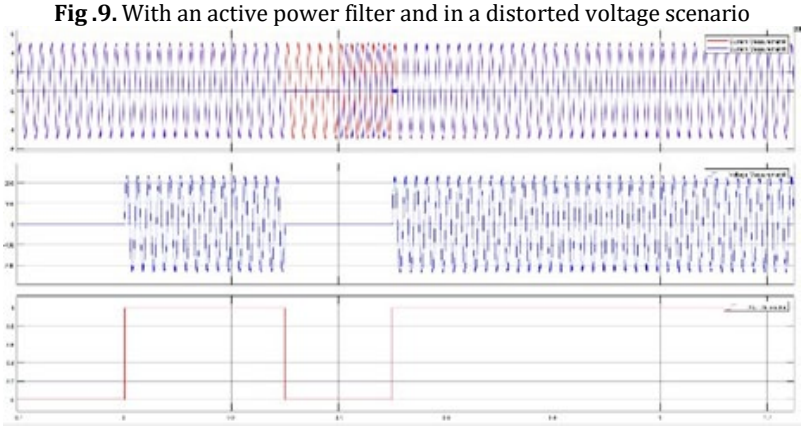

Fig.10. syncing, method shifting, and signals generation

without influencing the capacity to the family load. In addition, during the association with/detaching from the lattice, the framework current (i_g) is smooth.

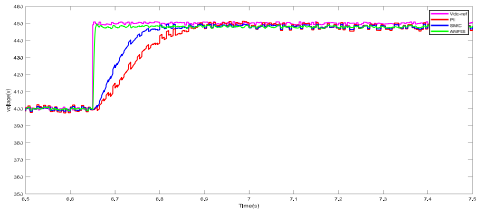

Fig.11 Study of Proportional Integral, Sliding Mode Control, and ANFIS controllers for DC-link voltage control Fig. 11 shows the dc-connect voltage (V_{dc}) guideline ability of the Proportional Integral regulator and Sliding Mode Control and ANFIS on the progression variation of 50V in ref dc-connect voltage (V^*). From Fig. 11, the ANFIS is quicker in managing the dc-interface voltage as thought about the SMC and PI control. Since the PV exhibit MPP activity relies upon the dc-interface voltage guideline at MPP voltage; the Photovoltaic module doesn't work at MPP because of the consistent state error in Proportional Integral regulator. Additionally, it likewise changes under the unexpected change in Electric vehicle current. Be that as it may, with SMC, the consistent state error is consistently zero and it additionally doesn't change with EV current change. In this manner, it generally works at MPP.

5. CONCLUSION

With the use of Insulated Gate Bipolar Transistor switch mode converters, a photovoltaic model, an electric vehicle charger, and a control system, an interconnected battery with a photovoltaic system, home load, and grid has been developed, with test results confirming continuous vehicle charging and home supply in both standalone and GCM modes of operation. Based on the outcome of these tests, this battery seems to be capable of charging electric vehicles, providing load requirements, and ensuring electric grid reliability. Vehicle-to-home function with less than 5% voltage THD and standalone performance with a photovoltaic system have also been shown. The test results show that utilizing the ANFIS controller, a seamless transition from standalone to GCM and vice versa is possible.

CONFLICT OF INTERESTS

None.

ACKNOWLEDGMENTS

None.

REFERENCES

J. R. Aguero, E. Takayesu, D. Novosel and R. Masiello, "Modernizing the Grid: Challenges and Opportunities for a Sustainable Future," *IEEE Power and Energy Magazine*, vol. 15, no. 3, pp. 74-83, May-June 2017.

D. Bowermaster, M. Alexander and M. Duvall, "The Need for Charging: Evaluating utility infrastructures for electric vehicles while providing customer support," *IEEE Electrifi. Mag.*, vol. 5, no. 1, pp. 59-67, 2017

X. Lu and J. Wang, "A Game Changer: Electrifying Remote Communities by Using Isolated Microgrids," *IEEE Electrifi. Mag.*, vol. 5, no. 2, pp. 56- 63, June 2017.

T. Ma and O. A. Mohammed, "Optimal Charging of Plug-in Electric Vehicles for a Car-Park Infrastructure," *IEEE Trans. Ind. Applicat.*, vol. 50, no. 4, pp. 2323-2330, July-Aug. 2014.

L. Cheng, Y. Chang and R. Huang, "Mitigating Voltage Problem in Distribution System With Distributed Solar Generation Using Electric Vehicles," *IEEE Trans. Sust. Ene*, vol. 6, no. 4, pp. 1475-1484, Oct. 2015.

S. J. Gunter, K. K. Afridi and D. J. Perreault, "Optimal Design of Grid- Connected PEV Charging Systems With Integrated Distributed Resources," *IEEE Trans. Smart Grid*, vol. 4, no. 2, pp. 956-967, 2013.

A. S. Satpathy, N. K. Kishore, D. Kastha and N. C. Sahoo, "Control Scheme for a Stand-Alone Wind Energy Conversion System," *IEEE Trans. Energy Conversion*, vol. 29, no. 2, pp. 418-425, June 2014.

F. Marra, G. Y. Yang, C. Træholt and E. Larsen, "EV Charging Facilities and Their Application in LV Feeders With Photovoltaics," *IEEE Trans. Smart Grid*, vol. 4, no. 3, pp. 1533-1540, Sept. 2013.

N. Saxena, I. Hussain, B. Singh and A. L. Vyas, "Implementation of a Grid-Integrated PV-Battery System for Residential and Electrical Vehicle Applications," *IEEE Trans. Ind. Electron.*, vol. 65, no. 8, pp. 6592-6601, Aug. 2018.
V. Monteiro, J. G. Pinto and J. L. Afonso, "Experimental Validation of a Three-Port Integrated Topology to Interface Electric Vehicles and Renewables With the Electrical Grid," *IEEE Trans. Industrial Informatics*, vol. 14, no. 6, pp. 2364-2374, June 2018.
V. T. Tran, K. M. Muttaqi and D. Sutanto, "A Robust Power Management Strategy With Multi-Mode Control Features for an Integrated PV and Energy Storage System to Take the Advantage of ToU Electricity Pricing," *IEEE Trans. Ind. App.*, vol. 55, no. 2, pp. 2110-2120, 2019.
A. Tazay and Z. Miao, "Control of a Three-Phase Hybrid Converter for a PV Charging Station," *IEEE Trans. Energy Conver.*, vol. 33, no. 3, pp. 1002-1014, Sept. 2018.
A. Verma, B. Singh, A. Chandra and K. Al-Haddad, "An Implementation of Solar PV Array Based Multifunctional EV Charger," in *IEEE Transpo.. Electrifi. Conf. and Expo (ITEC)*, Long Beach, CA, 2018, pp. 531-536.
M. Jafari, Z. Malekjamshidi, J. Zhu and M. Khooban, "Novel Predictive Fuzzy Logic-Based Energy Management System for Grid-connected and Off-grid Operation of Residential Smart Micro-grids," *IEEE Journal of Emerging and Selected Topics in Power Electronics*, Early Access.
T. He, D. D. Lu, L. Li, J. Zhang, L. Zheng and J. Zhu, "Model-Predictive Sliding-Mode Control for Three-Phase AC/DC Converters," *IEEE Trans. Power Electronics*, vol. 33, no. 10, pp. 8982-8993, Oct. 2018.